
Chapter 3

Numerical simulations: model setup and validation

Chapter 3

Numerical simulations: model setup and validation

3.1. Introduction

Numerical simulations have been carried out to study wave features prevailing along the Indian coast. Wave parameters obtained from the simulations are analysed to understand the phenomena associated with wave generation and dissipation in the Indian Ocean and coastal region. This chapter describes the model set up, calibration and validation using MIKE 21 model, and simulations using MM5 winds for the wind seas off Goa. Model set up consists: selection of model domain, generation of flexible mesh and gridded bathymetry, consideration of calibration parameters, initial/boundary conditions and wind input. Validation for model results was carried out wherever measurements are available within the selected domain. A sensitivity test with winds from various sources is also carried out to decide the accuracy of analysed winds used in the simulations.

3.2. Model setup

The model used to simulate waves over flexible mesh/gridded bathymetry is MIKE 21. The following sections describe the model set up in detail.

3.2.1. Model domain and bathymetry

In order to simulate waves in the Indian Ocean, a large domain, which ranges from 65° S to 30° N (latitude) and 20° E to 125° E (longitude) was selected. An unstructured triangulated mesh is generated with varying sizes of triangles (elements); 1.5° (south Indian Ocean), 0.75° (north Indian Ocean) and 0.25° (coastal regions). ETOPO5 bathymetry data obtained from NGDC (National Geophysical Data Center, Colorado, USA) is applied to deep water regions, whereas C-MAP data and improved bathymetry data sets of Sindhu et al. (2007) are applied to shallow water regions in the Indian Ocean, by interpolating them to each element in the flexible mesh bathymetry. The horizontal datum is referenced to World Geodetic System 1984 (WGS-84) and the vertical datum is referenced to Chart Datum (CD). Figure 3-1 shows the model domain, flexible mesh and bathymetry used for wave simulations in the Indian Ocean. The model used to simulate waves over flexible mesh bathymetry is MIKE 21 SW.

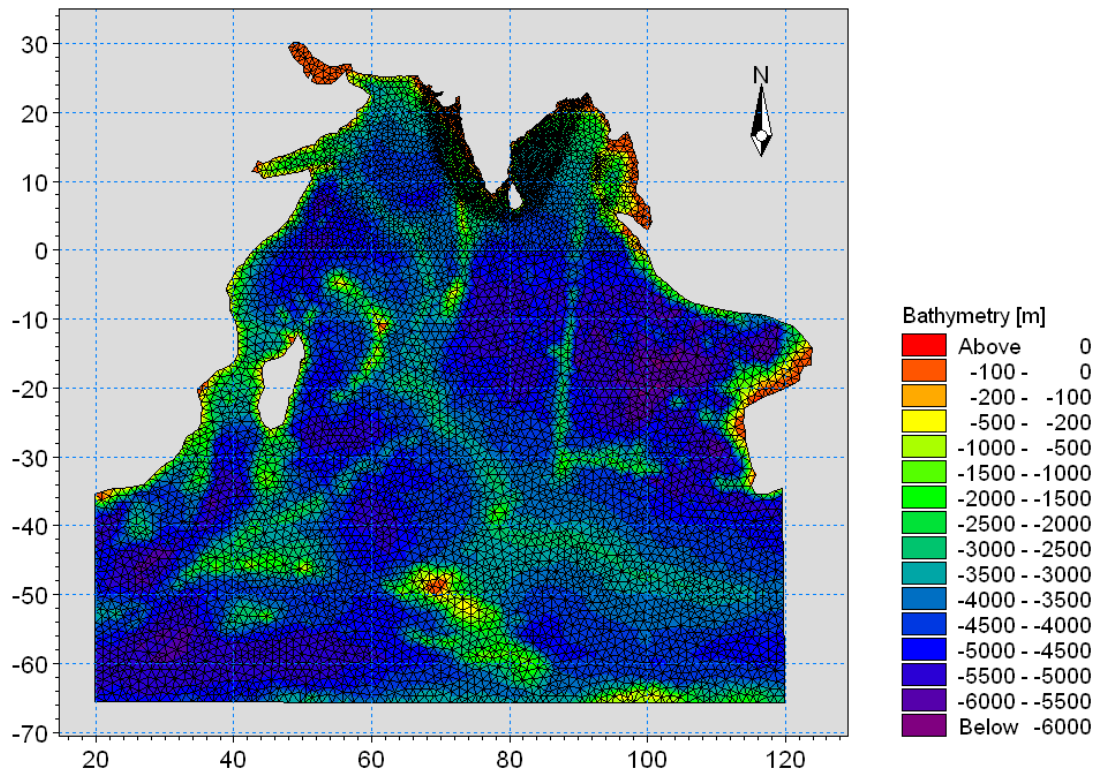


Figure 3-1. Model domain, bathymetry and flexible mesh used for wave simulations in the Indian Ocean.

Before switched over to MIKE 21 SW, the two-dimensional Offshore Spectral Wave model, MIKE OSW (DHI, 2001) was used to simulate the waves in the Indian Ocean over a rectangular grid bathymetry. Earlier, Vethamony et al (2006) used this model to simulate waves in the north Indian Ocean using MSMR (Multi-channel Scanning Microwave Radiometer) analysed winds. Since OSW has been replaced by SW, most of the offshore simulations in the present study have been carried out in SW, though some of the analysis was based on OSW results. Figure 3-2 shows the model domain and bathymetry used for OSW simulations in the Indian Ocean. The domain ranges from 5° S to 25° N and from 45° E to 100° E, and is divided into 40 x 74 grids in latitude and longitude, respectively with a grid spacing of 0.75° x 0.75°. The boundary along 5° S latitude was considered as open boundary, and all other boundaries were kept closed.

Local models were set up over fine resolution flexible mesh bathymetry at select nearshore regions along the east and west coasts of India. The select regions are Goa, Ratnagiri and Dwarka along the west coast, and Paradip and Dhamra along the east coast. Wave

measurements are available at these locations for validation. Figure 3-3 and Figure 3-4 show the model domain, bathymetry and triangulated mesh at locations along the west coast and east coast, respectively. Three open boundaries were made in all the model domains and utilized the boundary conditions obtained from the overall Indian Ocean model simulation results. The triangulated mesh sizes vary with respect to domains selected, and are listed below:

- i. off Goa: 15 km, 5 km, 2 km, 500 m, 300 m and 50 m. The 50 m size is considered in and around the breakwater area at Mormugao Port.
- ii. off Ratnagiri: 5 km, 1.5 km and 500 m.
- iii. off Dwarka: 2.5 km, 1.5 km and 500 m.
- iv. off Paradip: 2.5 km and 1.0 km.
- v. off Dhamra: 5 km, 1.5 km and 300 m.

MIKE 21 NSW has been used to simulate nearshore waves off Goa to demarcate of inland vessel's limit (IVL) off Mormugao port region. However, it has been replaced with SW in further simulations, as the later performs well compared to NSW. The bathymetry and model domain used for NSW simulations off Goa is shown in Figure 3-5.

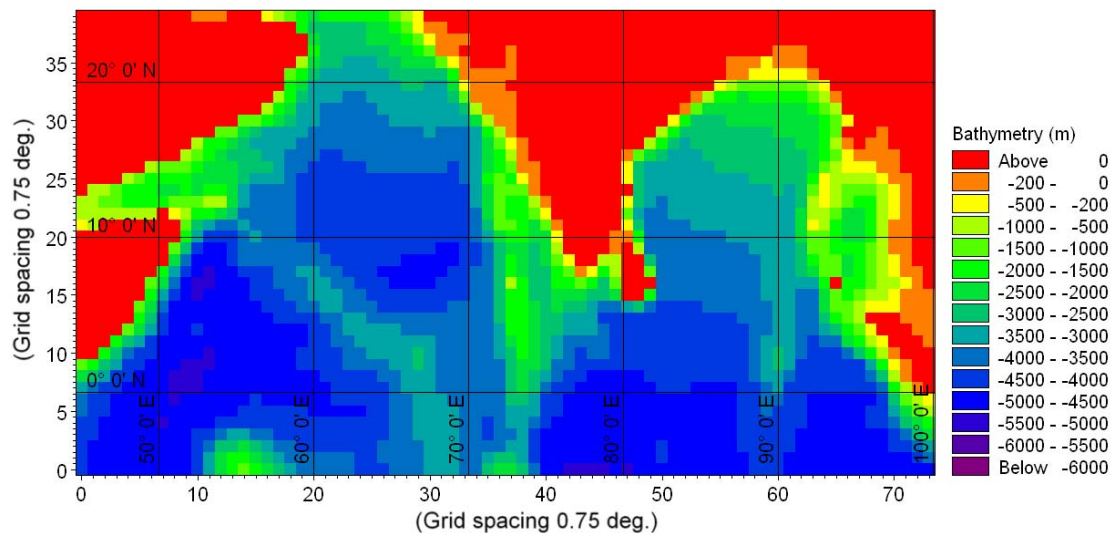


Figure 3-2. Model domain and bathymetry used for OSW simulations in the Indian Ocean.

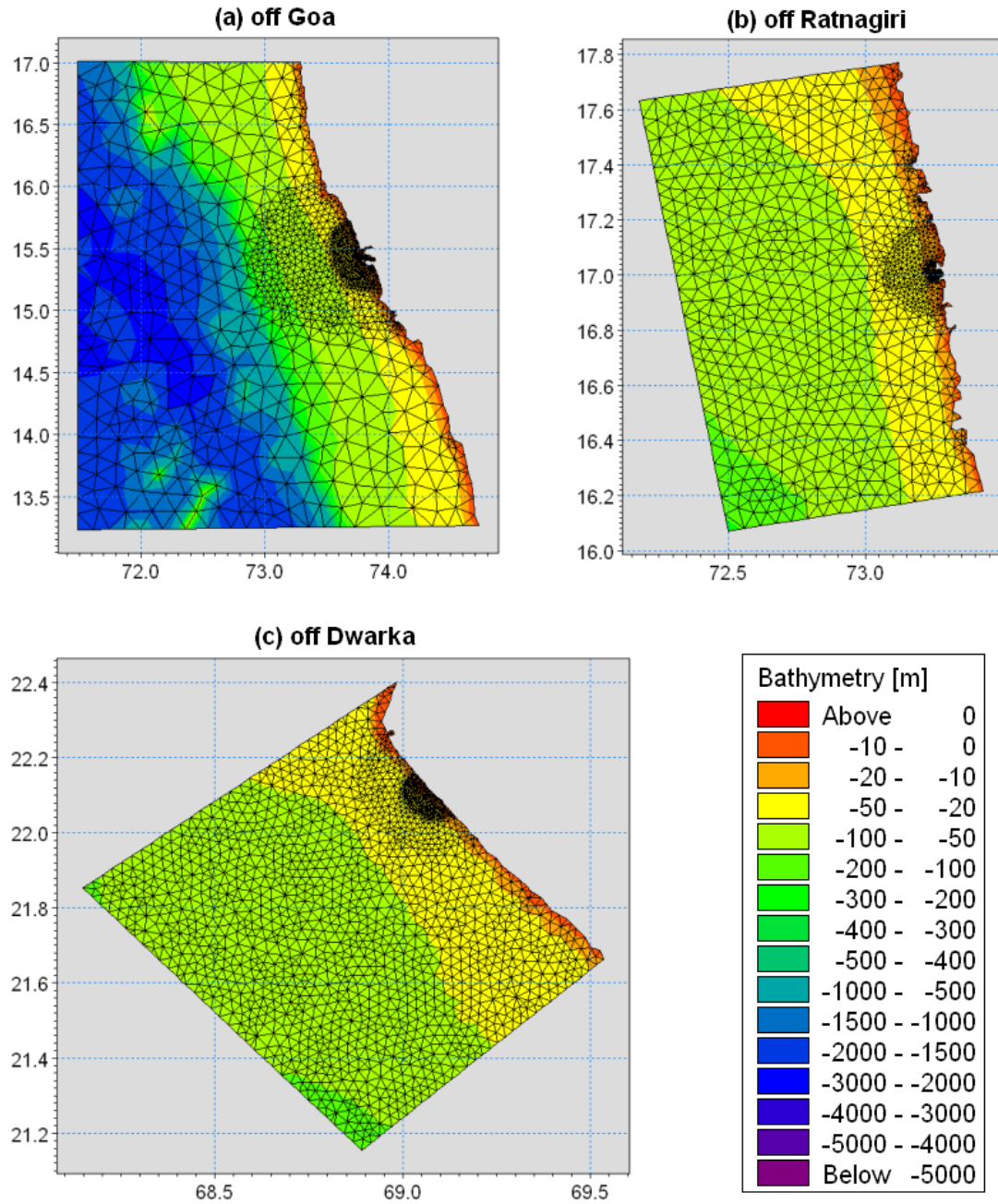


Figure 3-3. Domain, bathymetry and flexible mesh used for the local model (SW) simulations along the west coast of India: (a) off Goa, (b) off Ratnagiri and (c) off Dwarka.

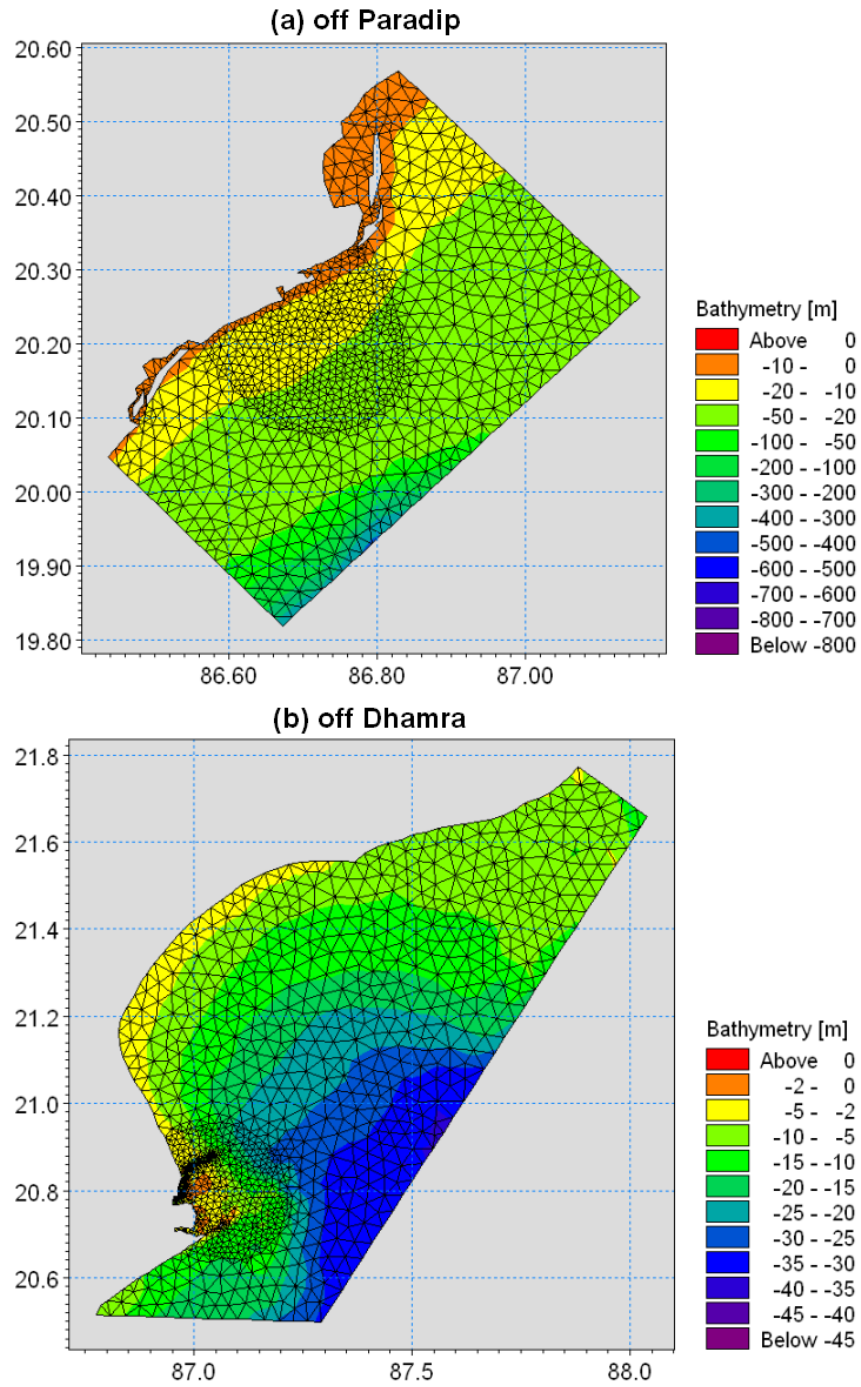


Figure 3-4. Domain, bathymetry and flexible mesh used for the local model (SW) simulations along the east coast of India: (a) off Paradip, (b) off Dhamra.

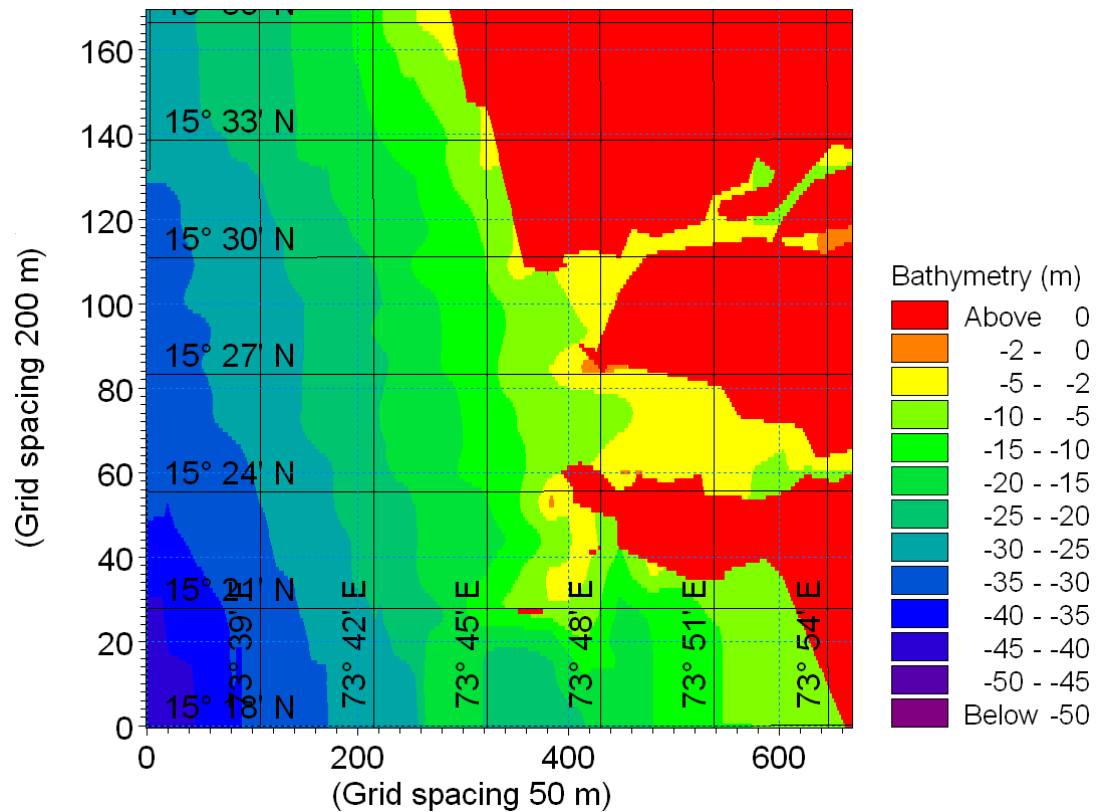


Figure 3-5. Domain and bathymetry used for the NSW simulations off Goa.

An overall wave transformation model was setup with fine resolution meshes in a single domain, specifically to study the wave transformation over a period of one year (Figure 3-6). Fine resolution meshes have been made for the regions Mumbai, Ratnagiri and Kochi along the west coast and Paradip, Visakapattinam and Nagappattinam along the east coast. The finest resolution considered is 500 m, and computational time is high.

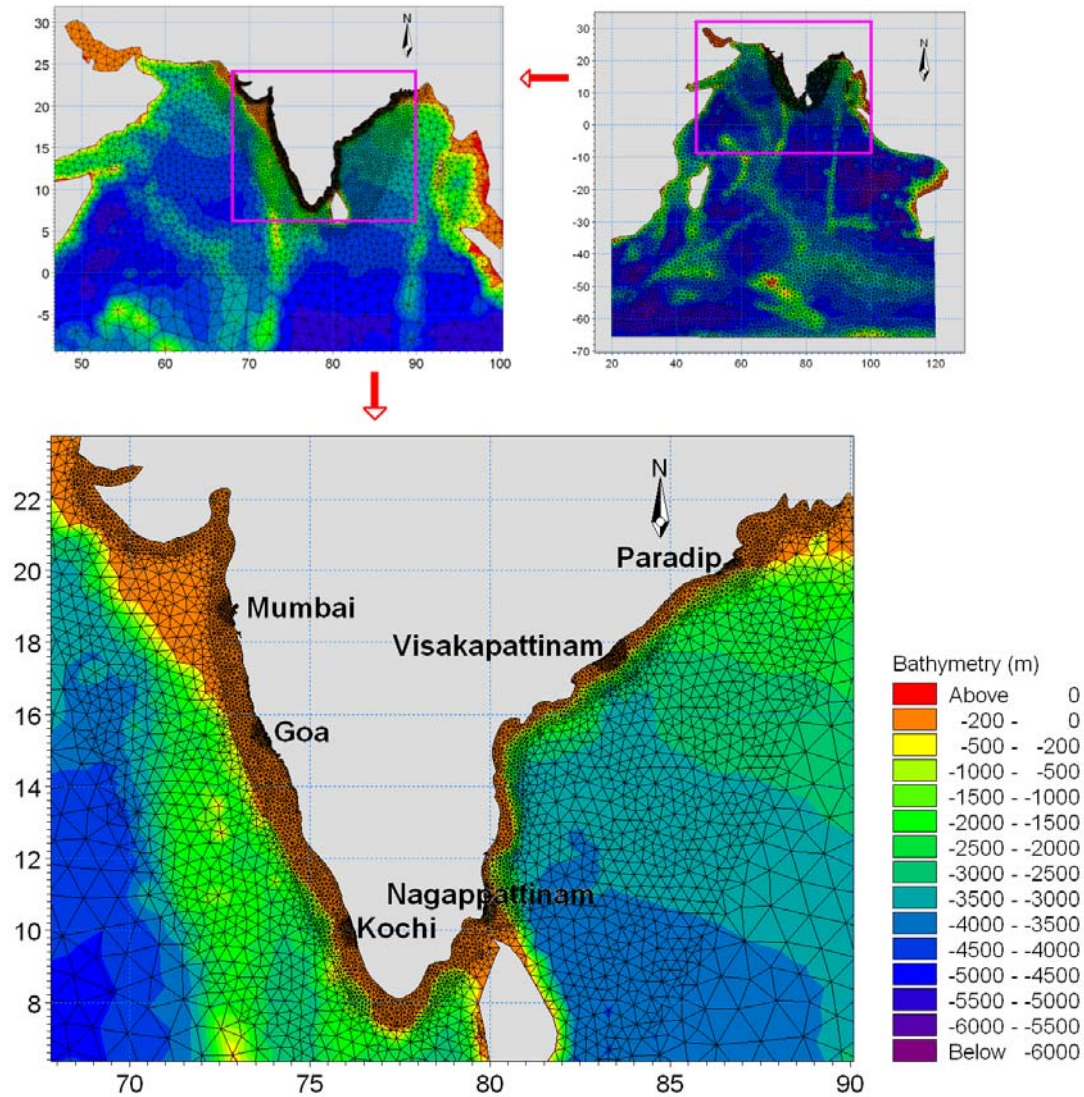


Figure 3-6. Bathymetry and flexible mesh used for SW simulations for wave transformation along the coast of India.

3.2.2. Basic formulations

Fully spectral formulations have been applied in the model set up. It is based on the wave action balance equation where the wave field is represented by the wave action density spectrum $N(\sigma, \theta)$. The independent phase parameters have been chosen as the relative (intrinsic) angular frequency, $\sigma=2\pi f$ and the direction of wave propagation, θ . The relation between the wave energy density spectrum $E(\sigma, \theta)$ and the wave action density spectrum is given by,

$$N(\sigma, \theta) = E/\sigma \quad \dots\dots\dots (3.1)$$

The spectral wave calculation is activated at a start time step relative to the start of the simulation specified.

The simulation time and accuracy can be controlled by specifying the order of the numerical schemes which are used in the numerical calculations. The schemes for discretization in the geographical domain and the spectral domain can be specified. In the present study, a low order fast algorithm has been used as the geographical space discretization. The dependent variable in the spectral mode is the directional-frequency wave action spectrum in each node point. Hence, the discretization has been made on frequency and direction. For frequency discretization, the logarithmic distribution has been considered, which is given by

$$f_n = f_0 c^n, \quad n = 1, 2, \dots \dots\dots (3.2)$$

where, f_n is the frequency, f_0 minimum frequency and c the frequency factor (= 1.1). The minimum frequency is set to 0.055 Hz and the number of frequencies is 25. For directional discretization, 360° rose has been considered. The number of directions is set to 16. For wind sea and swell separation, a dynamic threshold frequency scheme is applied by setting a maximum threshold frequency of 0.3 Hz.

The time integration is based on a fractional step approach. Firstly, a propagation step is performed calculating an approximate solution at the new time level by solving the basic conservation equations without the source functions. Secondly, a source function step is performed calculating the new solution from the estimated solution taking into account only the effect of the source functions. The propagation step is carried out by an explicit Euler scheme. To overcome the severe stability restriction, a multi-sequence integration scheme is employed following Vilsmeier and Hänel (1995). Here, the maximum time step is increased by locally employing a sequence of integration steps, where the number of levels (steps) may vary from element to element. The maximum number of levels in the propagation calculation is 32. The source integration step is carried out using the method of Komen et al. (1994) and Hersbach (1997) and the number of time steps in the source calculation is set as 1. A variable time step interval is used in the time integration of the governing equations. The time step is determined so that the CFL number is less than the maximum number of levels in all computational nodes. The number of levels (and thereby the local time step) for each element is then determined so that the local CFL number is

less than 1. The minimum and maximum time steps were set to 0.01 s and 1200 s respectively. The CFL number is defined as

$$CFL = \left| c_x \frac{\Delta t}{\Delta x} \right| + \left| c_y \frac{\Delta t}{\Delta y} \right| + \left| c_\sigma \frac{\Delta t}{\Delta \sigma} \right| + \left| c_\theta \frac{\Delta t}{\Delta \theta} \right| \dots\dots\dots (3.3)$$

where c_x , c_y , c_σ and c_θ are the propagation velocities of a wave group in the four-dimensional phase spaces x , y , σ and θ . Δx and Δy are characteristic length scale in the x - and y -directions for an element, $\Delta \sigma$ and $\Delta \theta$ are discrete intervals in the direction and frequency spaces and Δt is the time step interval.

3.2.3. Input parameters

Wind is the basic input parameter for wave simulation. Successful wave hindcast and forecast depend on accurate wind fields deduced from meteorological models and analysis. In the present study, NCEP winds, IFREMER/CERSAT blended winds, NCMRWF winds and QuikScat winds have been used. In the MIKE 21 SW simulations, these winds are directly used according to their temporal and spatial resolutions (as described in Sec 2.2.5 to Sec 2.2.8) over the Indian Ocean domain, whereas winds are spatially interpolated to the respective grids to apply in the MIKE 21 OSW simulations. Apart from these sources, AWS winds measured at coastal stations and MM5 winds simulated for the domain were also used for the nearshore wave simulations.

Global winds and MM5 winds are applied as vector components (in the form of u and v velocities) varying in time and space. For the air-sea interaction, a “coupled” formulation is applied according to the formulation of Komen et al (1994). It means the momentum transfer from the wind to the waves or drag depends not only on the wind but also on the waves. The applied background roughness Charnock parameter is 0.01. The Charnock parameter is defined as,

$$z_{ch} = g \cdot z_0 / u_*^2 \dots\dots\dots (3.4)$$

where u_* is the friction velocity and z_0 is the sea roughness.

The wind input source term is parameterized following Janssen's formulation (Komen et al., 1994). For a given wind speed and direction, the growth rate of waves of a given frequency and direction depends on the friction velocity, u_* , and sea roughness z_0 . In principle, if the sea roughness is known or assumed (e.g. the Charnock parameter may be assumed), the wind friction speed can be estimated using the logarithmic wind profile. Thus, the growth rate of waves due to wind input can be calculated. Komen et al. (1994)

made a formulation by assuming a dimensionless sea roughness (z_{ch}) of 0.0144, to fit the observations compiled by Plant (1982).

3.2.4. Energy transfer

The nonlinear energy transfer amongst the different wave components of a directional-frequency spectrum plays a crucial role for the temporal and spatial evolution of a wave field. A quadruplet-wave interaction, which is described by the accepted approximate Discrete Interaction Approximate (DIA) (Komen et al. (1994), has been applied in the present study. The quadruplet-wave interaction controls (i) the shape-stabilization of the high-frequency part of the spectrum, (ii) the downshift of energy to lower frequencies and (iii) frequency-dependent redistribution of directional distribution functions.

3.2.5. Calibration parameters

3.2.5.1. White capping

The source function describing the dissipation due to white-capping is based on the theory of Hasselmann (1974). With the description of wind input introduced by Janssen (1989), it was realized that the dissipation source function needs to be adjusted in order to obtain a proper balance between the wind input and the dissipation at high frequencies. The dissipation source function,

$$S_{ds}(\sigma, \theta) = -C_{ds}(\bar{k}^2 m_0)^2 \left\{ (1 - \delta) \frac{k}{\bar{k}} + \delta \left(\frac{k}{\bar{k}}\right)^2 \right\} \bar{\sigma} N(\sigma, \theta) \dots\dots\dots (3.5)$$

Where, C_{ds} and δ are calibration parameters. The values applied for C_{ds} and δ in the present study are 4.5 and 0.5 respectively. \bar{k} is the mean wave number and m_0 is the zeroth moment of the spectra.

3.2.5.2. Bottom friction

As waves propagate into shallow water, the orbital wave velocities penetrate the water depth, and the source function due to wave-bottom interaction becomes important. The dissipation source function is based on the quadratic friction law and linear wave kinematic theory (Johnson and Kofoed-Hansen, 2000).

$$S_{bot}(\sigma, \theta) = -C_f \frac{k}{\sinh 2kh} E(\sigma, \theta) \dots\dots\dots (3.6)$$

where C_f is a dissipation coefficient ($= f_w U_{bm}$), which depends on the hydrodynamic and sediment conditions. Here f_w is the wave friction factor and U_{bm} is the maximum near-bed particle velocity.

In the present study, the bottom friction is considered according to Nikuradse roughness, k_N . It is a calibration factor and the value applied in the present study is 0.04 m.

3.2.5.3. *Wave breaking*

Depth-induced breaking occurs when waves propagate into very shallow areas, and the wave height can no longer be supported by the water depth. The formulation of wave breaking is based on the breaking model by Battjes and Janssen (1978).

The source term due to depth-induced breaking can be written as,

$$S_{surf}(\sigma, \theta) = -\frac{\alpha Q_b \bar{\sigma} H_m^2}{8\pi} \frac{E(\sigma, \theta)}{E_{tot}} \dots \dots \dots (3.7)$$

where, α ($=1.0$) is a calibration constant, Q_b is the fraction of breaking waves, $\bar{\sigma}$ is the mean relative frequency, E_{tot} is the total wave energy and $H_m = \gamma d$ is the maximum wave height. Here, γ is the free breaking parameter (a wave height to depth ratio). The alpha (α) controls the rate of dissipation and is a proportional factor to the wave breaking source function. Kaminsky and Kraus (1993) found that γ values are in the range between 0.6 and 1.59 with an average of 0.79. In the present study, $\gamma = 0.8$ has been applied.

3.2.6. *Initial conditions*

The initial conditions are applied by calculating the spectra from empirical formulations. In the present study, JONSWAP fetch growth expression has been applied to calculate the spectra. The following values are used for various parameters:

maximum fetch length: 100 km; maximum peak frequency: 0.4 Hz; maximum Philip's constant: 0.0081; shape parameter, σ_a : 0.07; shape parameter, σ_b : 0.09; peakedness parameter, γ : 3.3 .

3.2.7. *Boundary conditions*

For wave simulations in the Indian Ocean, all the boundaries were closed assuming that the influence of wave energy into the Indian Ocean from the rest of the Oceans has negligible impact along the Indian coastal regions. It means, no waves enter the model domain through this boundary and the outgoing waves are fully absorbed. However, for wave simulations in the local models, the wave parameters obtained from the Indian Ocean model were applied as the boundary conditions. For this purpose, wind sea and swell parameters were extracted from the coarser model outputs at the open boundaries of the

local models. The integral parameters applied are significant wave height (m), peak wave period (s), mean wave direction (deg) and directional standard deviation (deg).

3.2.8. Output parameters

The basic outputs from the simulations are integral wave parameters and spectral parameters. The integral wave parameters obtained from the simulations are listed in Table 3-1. The integral parameters are determined for the total spectrum, for the wind sea part of the spectrum and for the swell part of the spectrum. The distinction between wind sea and swell are estimated using dynamic threshold frequency. Here, the swell components are defined as those components fulfilling the following wave-age based criterion,

$$\frac{U_{10}}{c} \cos(\theta - \theta_w) < 0.83 \dots\dots\dots (3.8)$$

Where, U_{10} is the wind speed, c the phase speed and θ and θ_w are the wave direction and wind direction, respectively.

The important integral parameters used in the present study are significant wave height (H_{m0}), peak wave period (T_p), mean wave period (T_{m02}), mean wave direction (θ_m) and directional standard deviation (DSD).

Significant wave height, $H_{m0} = 4\sqrt{m_0} \dots\dots\dots (3.9)$

Peak wave period, $T_p = 1/f_p \dots\dots\dots (3.10)$

The peak frequency f_p is calculated from the one-dimensional frequency spectrum using a parabolic fit around the discrete peak.

Mean wave period, $T_{02} = \sqrt{m_0/m_2} \dots\dots\dots (3.11)$

Mean wave direction, $\theta_m = 270 - \tan^{-1}(b/a) \dots\dots\dots (3.12)$

where, $a = \frac{1}{m_0} \int_0^{2\pi} \int_0^\infty \cos(270 - \theta) E(f, \theta) df d\theta \dots\dots\dots (3.13)$

$$b = \frac{1}{m_0} \int_0^{2\pi} \int_0^\infty \sin(270 - \theta) E(f, \theta) df d\theta \dots\dots\dots (3.14)$$

The directional standard deviation DSD is defined by,

$$DSD = 180/\pi \sqrt{2(1 - \sqrt{a^2 + b^2})} \dots\dots\dots (3.15)$$

One-dimensional and two-dimensional spectra are obtained from numerical simulations. Directional spectrum or frequency spectrum is one-dimensional, whereas directional-

frequency spectrum is two-dimensional. The directional energy spectrum is obtained by integration over the discretized frequencies and, frequency energy spectrum is obtained by integration over the discretized directions. However, the 2D spectrum is obtained by integration over the discretized frequencies.

Table 3-1. Integral wave parameters obtained from wave simulations

Wave parameters	Symbol	SI unit
Significant wave height	H_{m0}	M
Maximum wave height	H_{max}	M
Peak wave period	T_p	S
Mean wave period	T_{01}	S
Mean wave period (Zero-crossing wave period)	T_{02}	S
Wave energy wave period	T_{-10}	S
Peak wave direction	θ_p	°N
Mean wave direction	θ_m	°N
Directional standard deviation	DSD	°
Wave velocity components	$H_{m0} \cdot \cos(\theta_m)$ $H_{m0} \cdot \sin(\theta_m)$	m/s
Radiation stresses	S_{xx}, S_{xy}, S_{yy}	m^3/s^2
Particle velocities	$U_{max}(z=-d),$ $U_{max}(z=0), W_{max}(z=0),$ $U_{max}(z=z_0), W_{max}(z= z_0)$	m/s

3.3. Model validation

Model results have been validated with measurements at one deep water location and two nearshore locations in the Indian Ocean. The measurement locations are DS1 (deep water), B1 and B8 (nearshore regions) as shown in Figure 2-1. Continuous 16 months time series data are available at B1, whereas 9 months data were available at DS1 and B8. In addition to DS1 data, Jason-1 significant wave heights at two deep water locations (in the Arabian Sea and Bay of Bengal) have been used to compare with modelled significant wave heights.

3.3.1. Validation at deep water locations

Measured wave data at DS1 is available for the period Jan. – Sep. 2001. Hence, the wave simulation has been carried out for the Indian Ocean using NCEP winds for the above period. The simulated wave parameters have been extracted at location DS1 and compared with measured parameters. Figure 3-7 shows the comparison between measured and modelled wave parameters. The modelled H_s and T_m show close match with the measured wave parameters. The extreme waves observed during the study period are well reproduced in the simulations.

The statistical parameters estimated between measured and modelled wave parameters at DS1 are listed in Table 3-2. Measured and modelled H_s and T_m are well correlated. The correlation coefficient of H_s and T_m are 0.96 and 0.85, respectively. There is no marginal bias between measured and modelled H_s , however, the r.m.s. error is 0.37 m. The mean wave period is slightly under estimated (bias = 0.32 s) and the corresponding r.m.s. error is 0.8 s. The scatter indices estimated for H_s and T_m are 0.2 and 0.14, respectively, which shows good linear fit between measured and modelled parameters. It is evident from the scatter plots (Figure 3-8) that the scatter points of H_s and T_m are linearly well packed. The statistical parameters confirm the excellent performance of the model and reliability of the simulation results.

Waves simulated using NCEP winds of 2005 are compared with Jason-1 data at two deep water locations: one in the Arabian Sea (G1) and another in the Bay of Bengal (P1). The geographical co-ordinates of G1 is 69° E, 15° N and that of P1 is 91° E, 18° N (Figure 2-3). The corresponding water depths are 3800 m and 2200 m at G1 and P1, respectively. Comparison between Jason-1 and model significant wave heights are shown in Figure 3-9. It shows that the modelled significant wave heights match very well with the remotely sensed observations (Jason-1). For larger waves, an underestimation has been observed in

the model significant wave heights. The gaps seen in Jason-1 H_s curve indicate missing values.

Table 3-3 shows the statistical parameters calculated between Jason-1 and model significant wave heights at locations G1 and P1. Good correlation is found between the two at both the locations with correlation coefficients 0.96 and 0.90 at G1 and P1, respectively. There is a slight overestimation of 0.12 m at G1 and an underestimation of 0.07 m at P1. The r.m.s. error calculated at G1 and P1 are 0.44 m and 0.31 m, respectively. The scatter indices (SI) calculated at G1 and P1 are 0.28 and 0.21, respectively. Again the statistical parameters show the reliability of the wave model used, as well as the use of altimeter data for comparison/validation.

Figure 3-10 shows the scatter between Jason-1 and model significant wave heights at G1 and P1. It is clear that the scatter is moderately narrow at both the locations, even though there is slight over estimation at G1 and an under estimation at P1. This shows that the model performs well at deep waters both in the Arabian Sea and the Bay of Bengal.

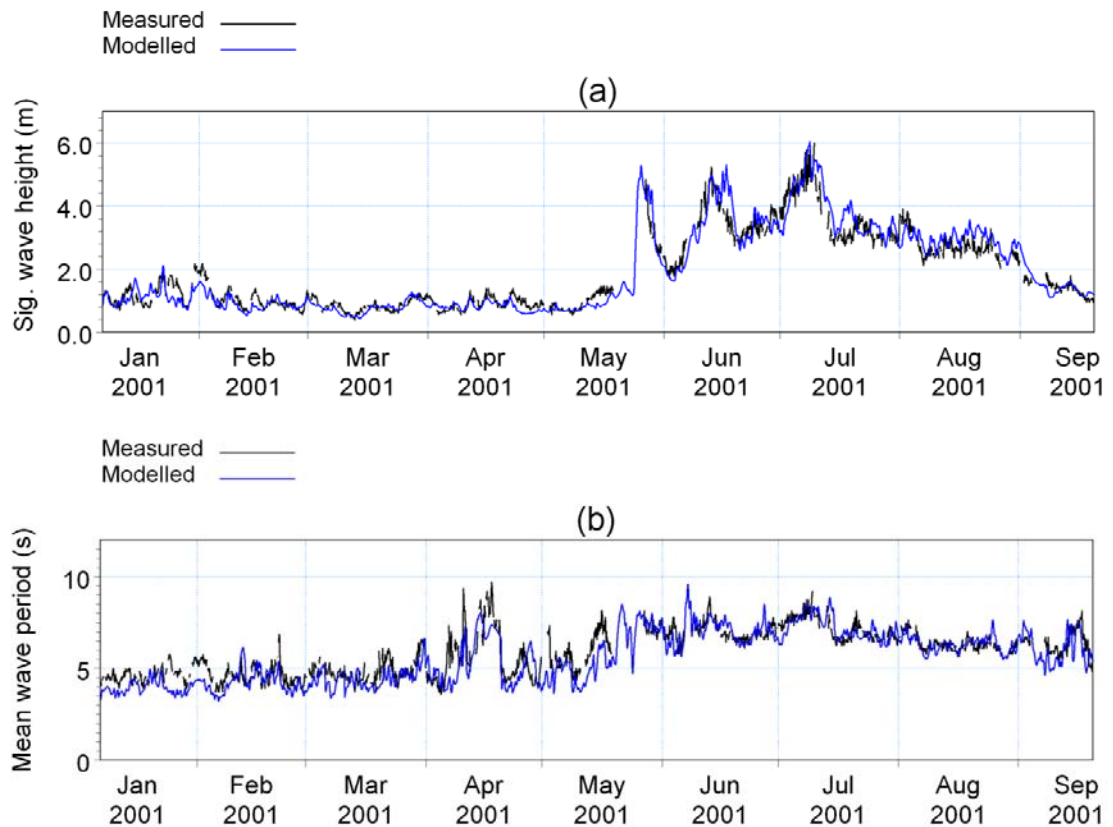


Figure 3-7. Comparison between measured and modelled wave parameters at DS1: (a) significant wave height and (b) mean wave period.

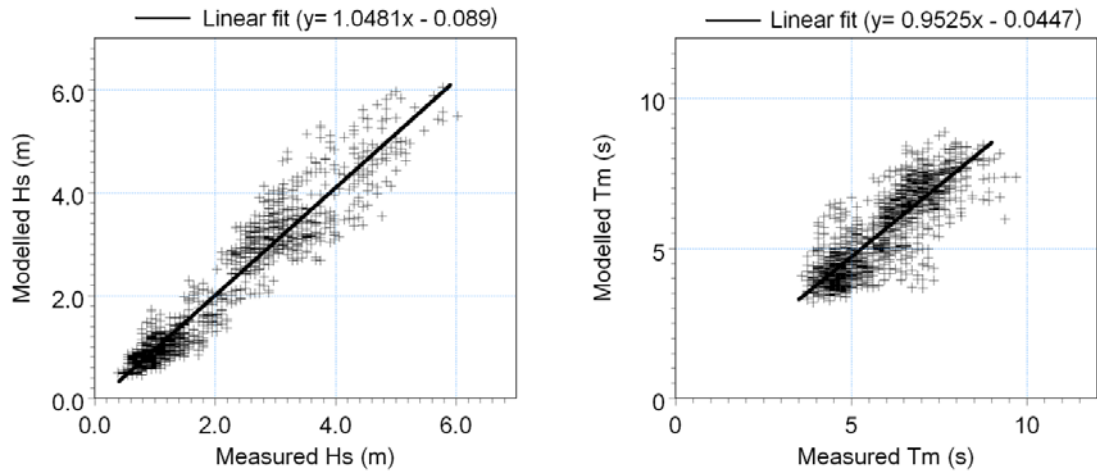


Figure 3-8. Scatter between measured and modelled H_s and T_m at DS1.

Table 3-2. Statistical parameters estimated between measured and model wave parameters at DS1.

Parameters	Correlation coefficient	Bias	r.m.s. error	Scatter Index
H_s (m)	0.96	0.00	0.37	0.20
T_m (s)	0.85	-0.32	0.80	0.14

Table 3-3. Statistical parameters estimated between Jason-1 and model significant wave heights at G1 and P1.

Location	Correlation coefficient	Bias (m)	r.m.s. error (m)	Scatter Index
G1 (off Goa)	0.96	0.12	0.44	0.28
P1 (off Paradip)	0.90	-0.07	0.31	0.21

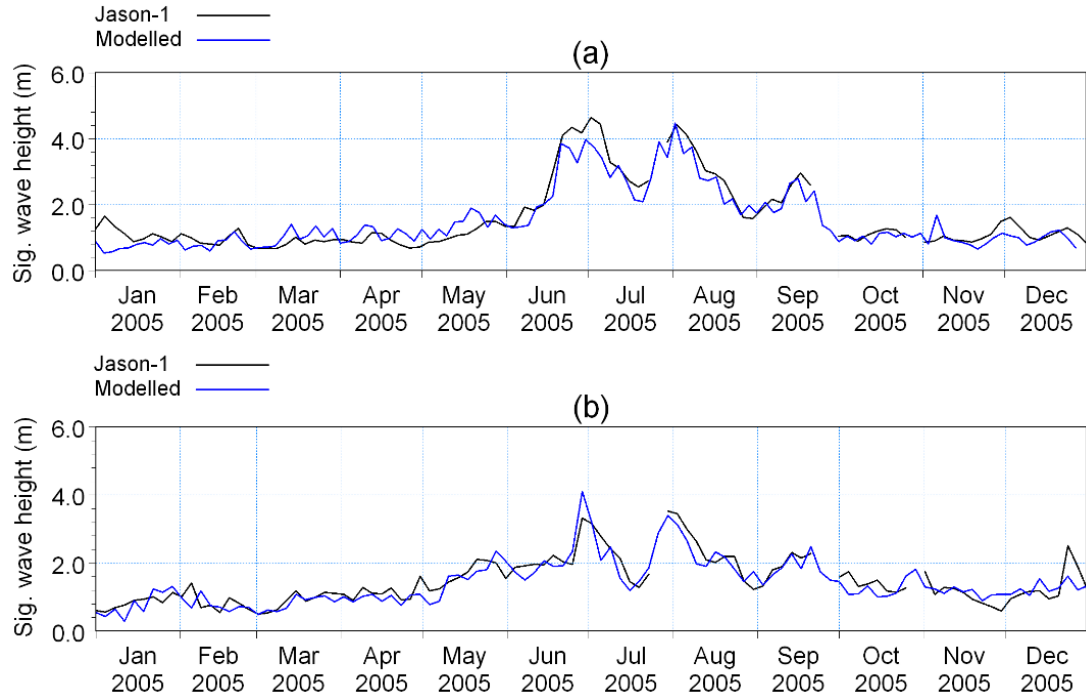


Figure 3-9. Comparison between Jason-1 and modelled H_s off: (a) Goa (at G1) and (b) Paradip (at P1).

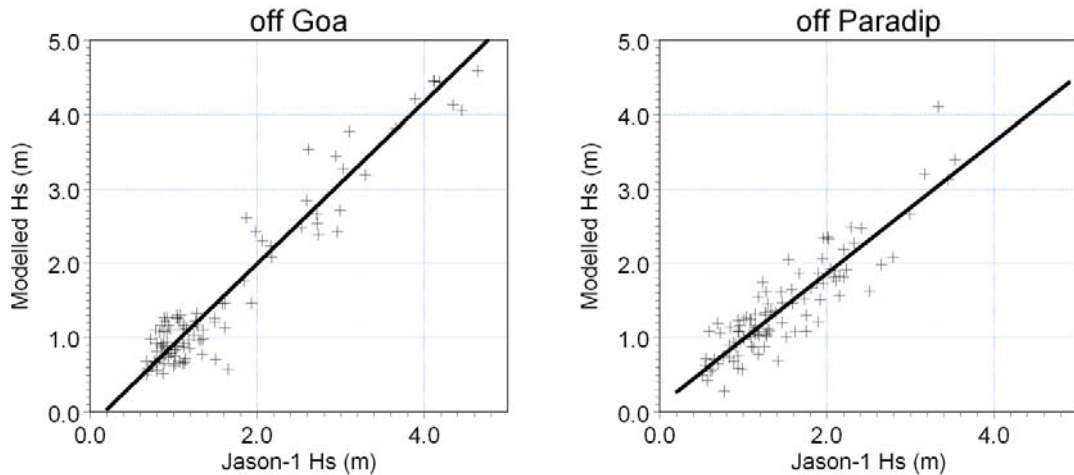


Figure 3-10. Scatter between Jason-1 and modelled H_s at G1 (off Goa) and P1 (off Paradip).

3.3.2. Validation at nearshore regions

The two select nearshore locations are B1 (off Goa) and B8 (off Paradip) as shown in Figure 2-1. Measurements are available during Feb 1996 - May 1997 at B1 and during May 1996 - Jan 1997 at B8. Wave simulations have been carried out using NCEP winds

during 1996 – 1997. The simulated wave parameters have been extracted at the above locations and compared with the measurements.

Figure 3-11 and Figure 3-12 show the comparison between measured and model wave parameters at locations B1 and B8, respectively. Model wave parameters show very good match with measured wave parameters, especially with significant wave height and wave direction at both the locations. The comparison of mean wave period is good at B1 and moderately good at B8.

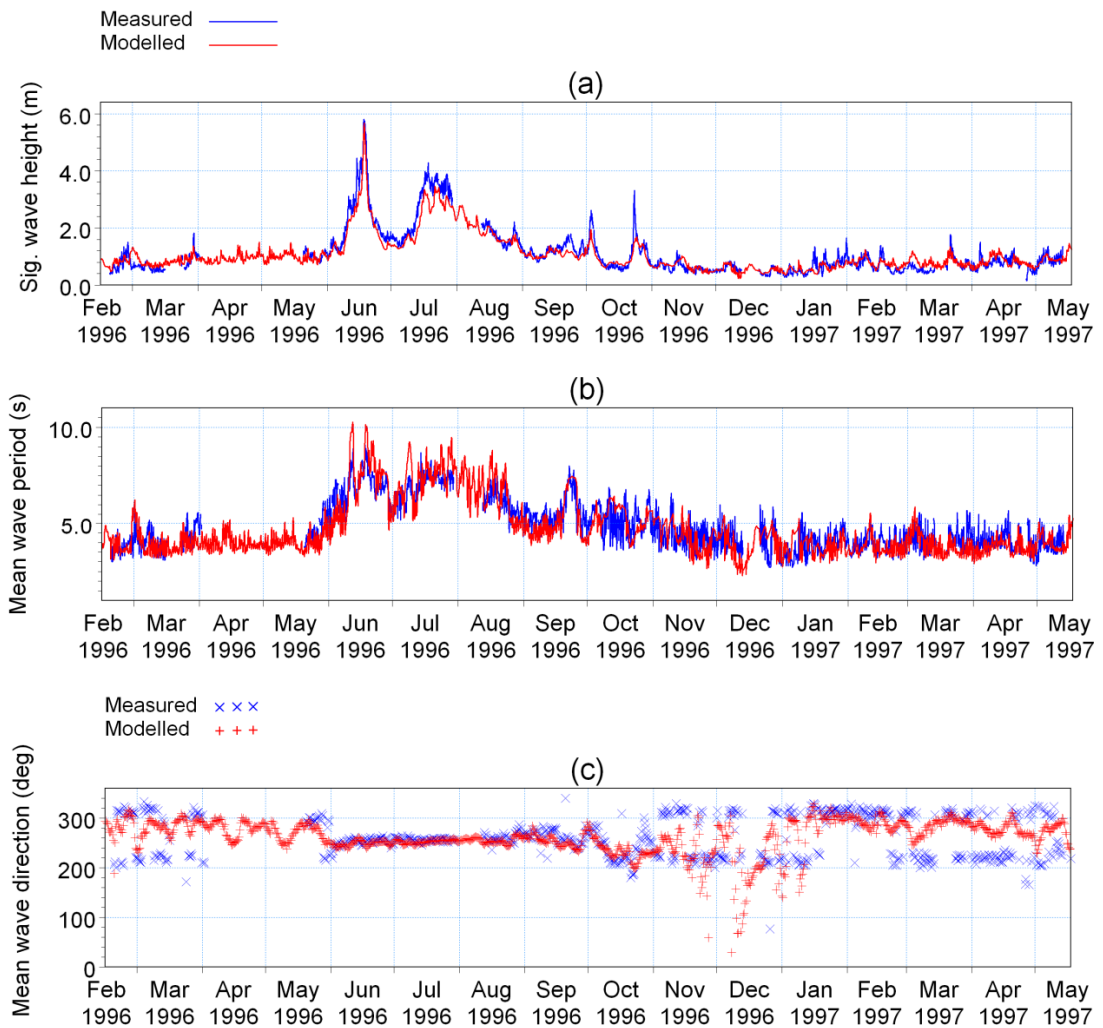


Figure 3-11. Comparison between measured and modelled wave parameters at B1 (off Goa): (a) significant wave height, (b) mean wave period and (c) mean wave direction.

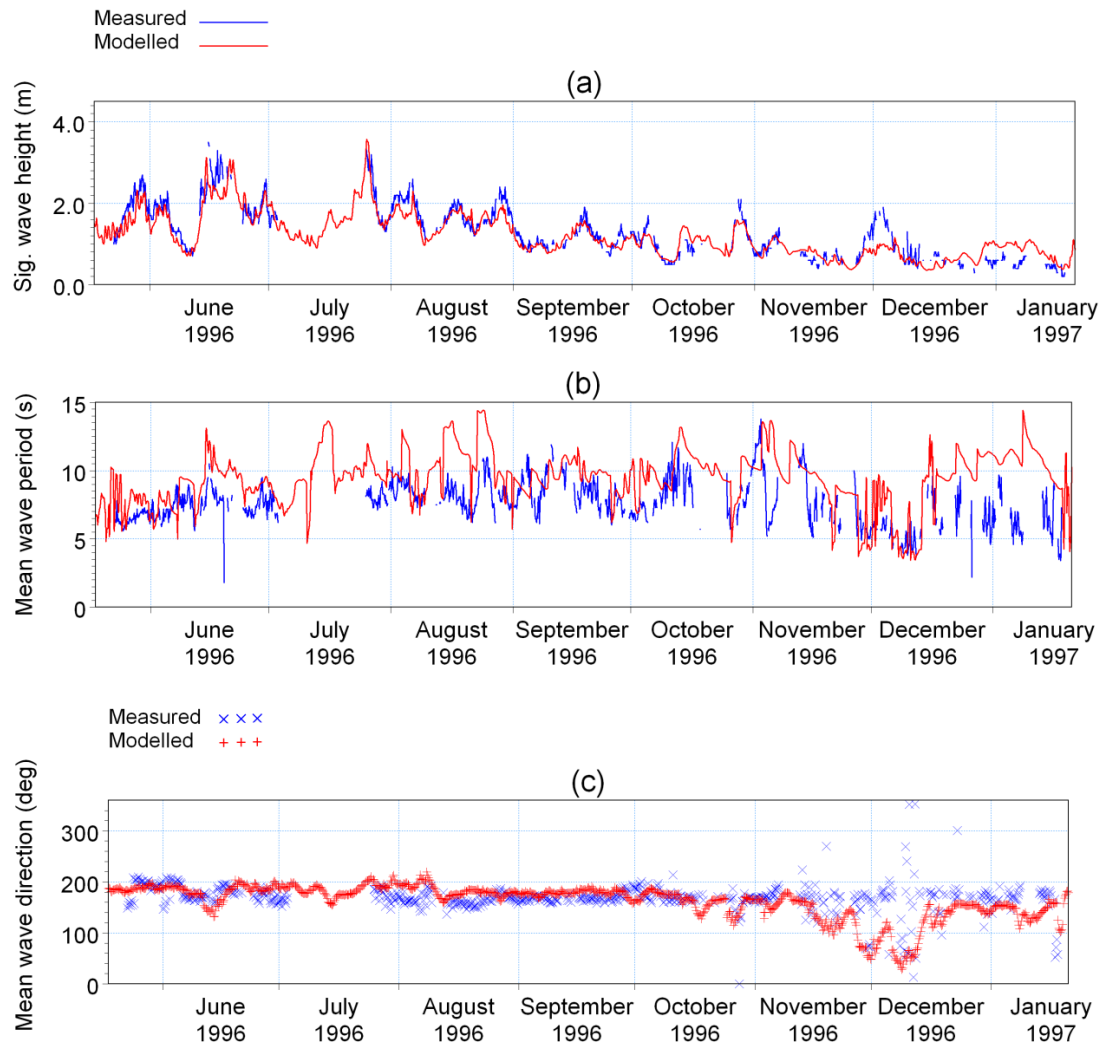


Figure 3-12. Comparison between measured and modelled wave parameters at B8 (off Paradip): (a) significant wave height, (b) mean wave period and (c) mean wave direction.

The statistical analysis of measured and modelled wave parameters have been made separately for wave, swell and wind sea at locations B1 and B8, which are listed in Table 3-4, respectively. Wave and swell are well predicted at both the locations, and not, the wind sea (moderately good). The moderate comparison of winds seas is due to the fact that coarse resolution wind input is applied to the wave model (explained in chapter 4). The correlation coefficients of significant heights of wave, swell and wind sea at location B1 are 0.96, 0.93 and 0.64, respectively, whereas those at B8 are 0.90, 0.84 and 0.63 for wave, swell and wind sea, respectively. The waves and swells are least biased at both the locations; very marginal overestimation in waves (0.06 m and 0.07 m for H_s and 0.1 s and

0.6 s for T_m at B1 and B8, respectively) and underestimation in swells (0.07 m and 0.04 m for H_s and 0.2 s and 0.52 s for T_m at B1 and B8, respectively). The r.m.s. error calculated for H_s (for wave and swell) are in the range of 0.29 - 0.36 m at both the locations. The r.m.s. error in period is low for resultant T_m (between 0.8 – 1.24 s) and larger for swell T_m (between 2.15 – 2.5 s).

The scatter indices are 0.25 and 0.22 for resultant H_s and 0.39 and 0.31 for swell H_s at B1 and B8, respectively. Similar results are observed for resultant T_m (0.17 and 0.22 at B1 and B8, respectively) and swell T_m (0.32 and 0.24 at B1 and B8, respectively). This indicates that the waves are least scattered and swells are moderately scattered. Figure 3-13 and Figure 3-14 show the scatter between measured and modelled wave parameters at locations B1 and B8, respectively. The points are linearly scattered for the waves and swells at B1 and B8, indicating that match is good between measured and modelled wave and swell parameters. The significant swell heights are also linearly correlated, though the mean swell periods show large deviations. The wind sea parameters other than H_s are widely scattered.

Table 3-4. Statistical parameters estimated between measured and model wave parameters at B1 (off Goa) and B8 (off Paradip).

Location	Parameters	Resultant wave		Swell		Wind sea	
		H_s (m)	T_m (s)	H_s (m)	T_m (s)	H_s (m)	T_m (s)
B1	Correlation coefficient	0.96	0.83	0.93	0.45	0.64	0.28
	Bias	0.06	0.1	-0.07	-0.2	0.31	0.3
	r.m.s. error	0.29	0.8	0.36	2.5	0.46	1.6
	Scatter Index	0.25	0.17	0.39	0.32	0.7	0.49
B8	Correlation coefficient	0.9	0.65	0.84	0.68	0.63	0.37
	Bias	0.07	0.6	-0.04	-0.52	0.15	-0.32
	r.m.s. error	0.29	1.24	0.32	2.15	0.12	1.69
	Scatter Index	0.22	0.22	0.31	0.24	0.61	0.43

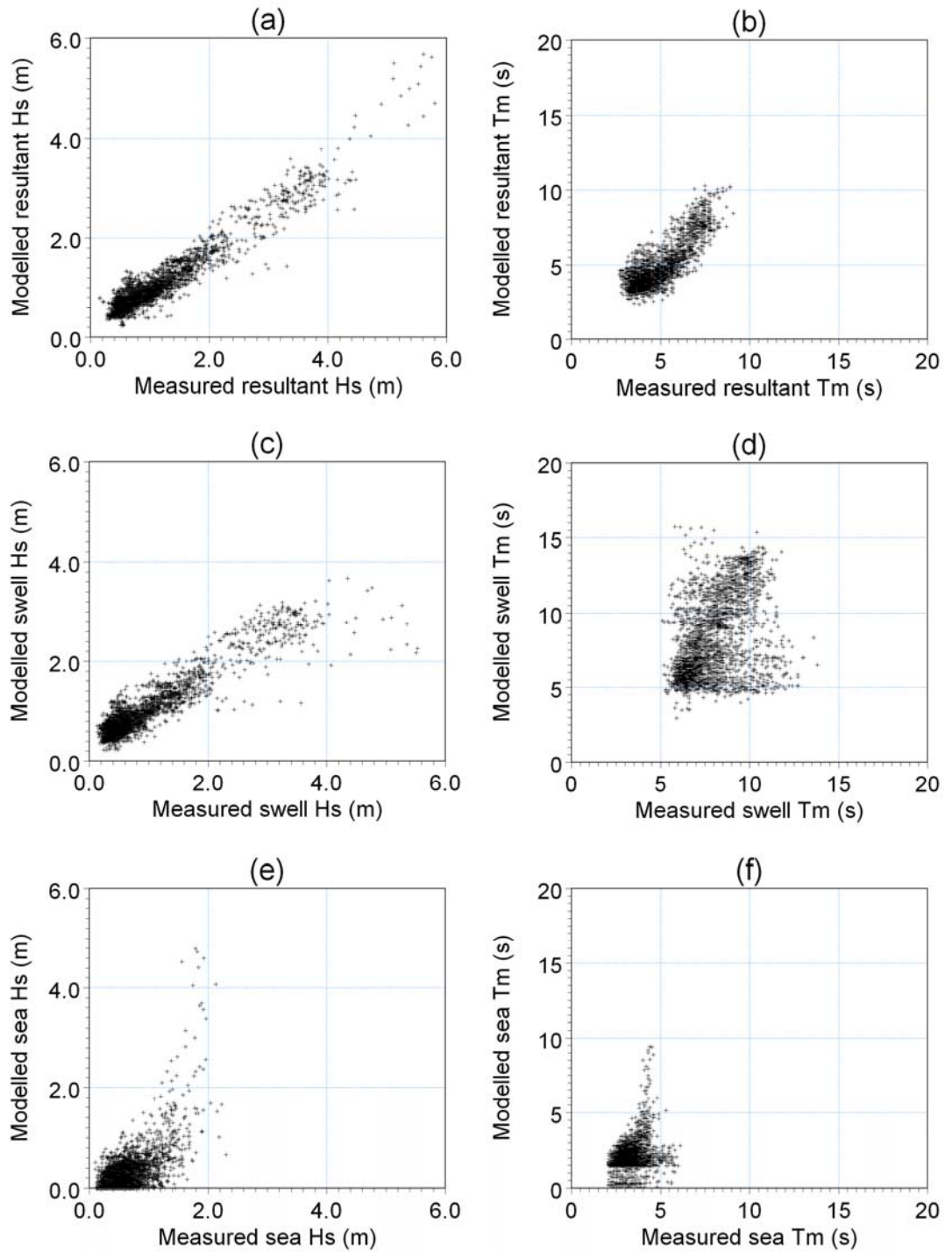


Figure 3-13. Scatter between measured and modelled wave parameters at B1 (off Goa): (a) resultant H_s , (b) resultant T_m , (c) swell H_s , (d) swell T_m , (e) wind H_s sea and (f) wind sea T_m .

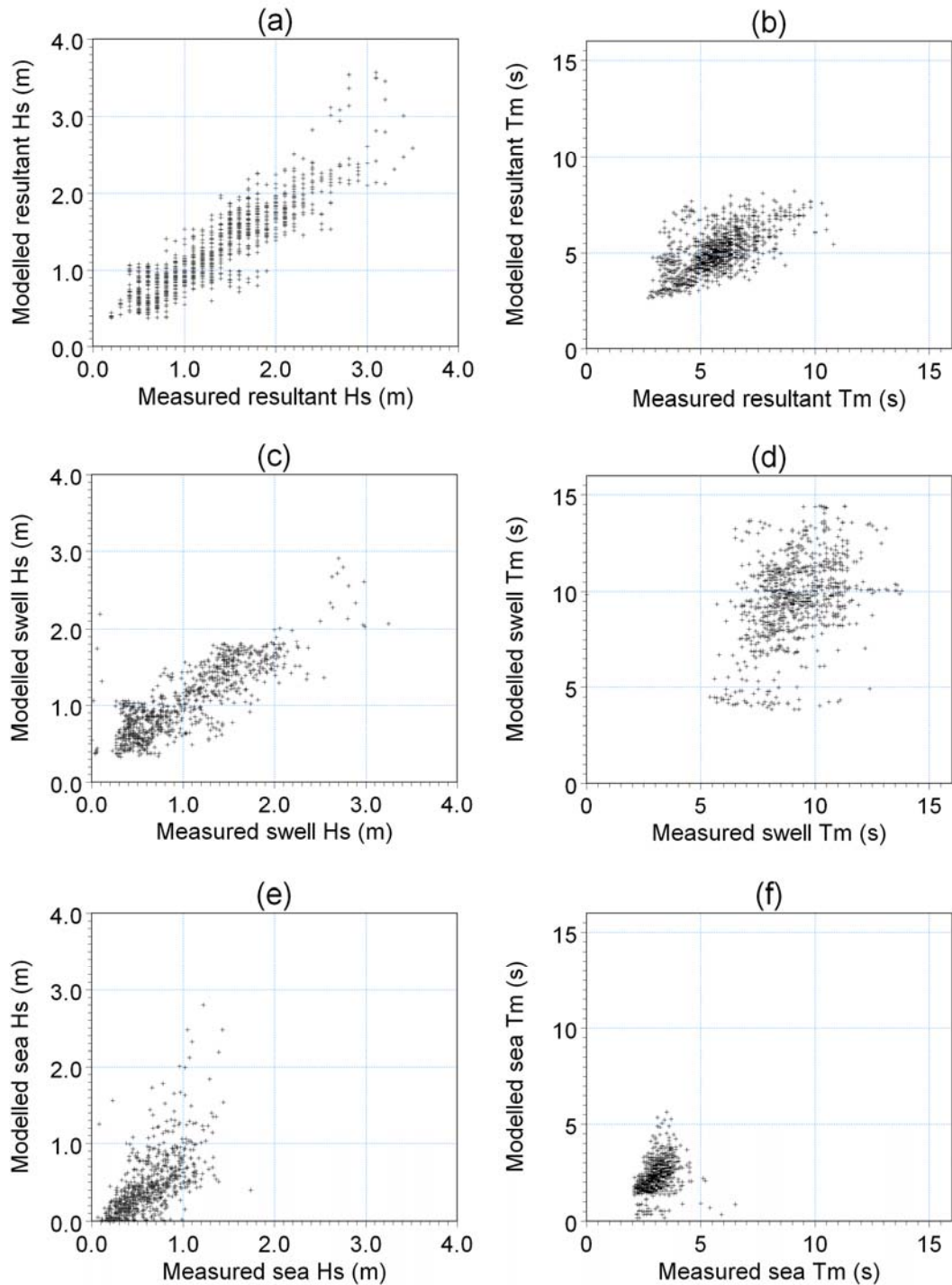


Figure 3-14. Scatter between measured and modelled wave parameters at B8 (off Paradip): (a) resultant H_s , (b) resultant T_m , (c) swell H_s , (d) swell T_m , (e) wind sea H_s and (f) wind sea T_m .

3.3.3. Sensitivity test

The model sensitivity of wave predictions using various wind inputs has been tested as wind is one of the basic input parameters which decide the accuracy of wave prediction. NCEP, IFREMER/CERSAT blended and QuikScat winds were applied to the simulations. The modelled wave parameters have been extracted at location B2 (off Goa) and compared with measurements available during 01 – 21 May 2005 at B2 (for every 1 hour). Statistical parameters such as correlation coefficient, bias, r.m.s. error and scatter index were also estimated.

Statistical parameters estimated between measured and modelled wave parameters at B2 are listed in Table 3-5. A good match is obtained for the simulation results using NCEP and blended winds, and match is relatively poor for QuikScat winds. Since, temporal resolution of the QuikScat winds is coarse (twice daily), the diurnal features along the coast, especially wind waves generated by the sea breeze and land breeze system, could not be reproduced well by the model.

Correlation coefficient and bias of H_s and T_m corresponding to NCEP and blended winds are nearly the same (correlation coefficients of H_s are 0.75 and 0.74, respectively and biases are 0.04 m and 0.09 m, respectively). Correlation coefficients of T_m corresponding to NCEP and blended winds are 0.63 and 0.59, and biases are 0.56 s and 0.47 s, respectively. T_m corresponding to QuikScat winds is poorly correlated (0.20), even though correlation of H_s is moderately good (0.64). The low scatter indices for all cases indicate that there is good linear fit between the measured and modelled parameters.

Since, NCEP winds and blended winds reproduced the near real waves in the simulations, these winds can be chosen for accurate wave predictions in the Indian Ocean. In the sensitivity test, a short duration data has been chosen (01 – 21 May 2005) to calculate the accuracy of wave prediction. However, better results could be obtained with long term observations. Since, the spatial resolution of blended winds is finer ($0.25^\circ \times 0.25^\circ$), characteristics of coastal winds could be incorporated for better wave prediction is expected near the coast.

Table 3-5. Statistical parameters estimated between measured and modelled (using NCEP, Blended and QuikScat winds) wave parameters at B2.

Statistical parameters	NCEP		Blended		QuikScat	
	H_s (m)	T_m (s)	H_s (m)	T_m (s)	H_s (m)	T_m (s)
Correlation coefficient	0.75	0.63	0.74	0.59	0.64	0.20
Bias	0.04	0.56	0.09	0.47	-0.02	0.55
r.m.s. error	0.12	0.75	0.15	1.04	0.11	0.83
Scatter Index	0.15	0.18	0.20	0.25	0.14	0.20

3.4. Simulations using MM5 winds

MM5 winds have been used to simulate wind seas off Goa (local domain) during May 2005, to study wind sea characteristics during pre-monsoon season. Another simulation has been carried out for the local domain considering the wave parameters extracted (at the boundaries of local domain) from the Indian Ocean model as boundary conditions and MM5 winds as input to simulate waves off Goa. The aim of this work is to make use of fine resolution MM5 winds in wave simulations to study coastal wave features due to coastal wind systems.

The wind seas simulated using MM5 winds have been validated with measurements at locations B2 and B3. For this purpose, wind sea and swell parameters at B2 and B3 are separated from the measured wave spectra as described in Sec 2.3.1 (Chapter 2). Figure 3-15 and Figure 3-16 show the comparison between measured and modelled wind sea parameters at B2 and B3, respectively. Modelled wind sea parameters show very good match with measurements. The diurnal pattern of wind seas is well reproduced in the model.

Statistical parameters estimated between measured and modelled wind sea parameters at B2 and B3 are listed in Table 3-6. There is good correlation between measured and modelled wind sea H_s , however, moderate correlation has been obtained between measured and modelled T_m . Correlation coefficients of H_s are 0.70 and 0.73 at B2 and B3, respectively. Biases are less (< 0.1 m for H_s and < 0.5 s for T_m), even though wind sea H_s

and T_m are underestimated by the model. The r.m.s. errors are upto 0.16 m for H_s and 0.55 s for T_m . All the statistical estimates are well within the acceptable limits for the waves.

Figure 3-17 and Figure 3-18 show the scatter between measured and modelled wind sea H_s and T_m at B2 and B3, respectively. There is a good linear fit for H_s , even though a few points are widely scattered. The scatter points of T_m are closely packed with most of the points centered between 2 and 3 s. In fact, these are the wind sea periods exist along the coastal region off Goa during pre-monsoon season.

The wind seas simulated using MM5 winds have been further utilised to study the diurnal variations associated with sea breeze-land breeze systems over the Goa coast during pre-monsoon season (May 2005). The results are discussed in Chapter 4.

Table 3-6. Statistical parameters estimated between measured and modelled wind sea parameters at B2 and B3.

Location	Parameters	Wind sea	
		H_s (m)	T_m (s)
B2	Correlation coefficient	0.70	0.39
	Bias	0.09	0.40
	r.m.s. error	0.16	0.52
	Scatter Index	0.30	0.17
B3	Correlation coefficient	0.73	0.37
	Bias	0.03	0.44
	r.m.s. error	0.12	0.55
	Scatter Index	0.26	0.18

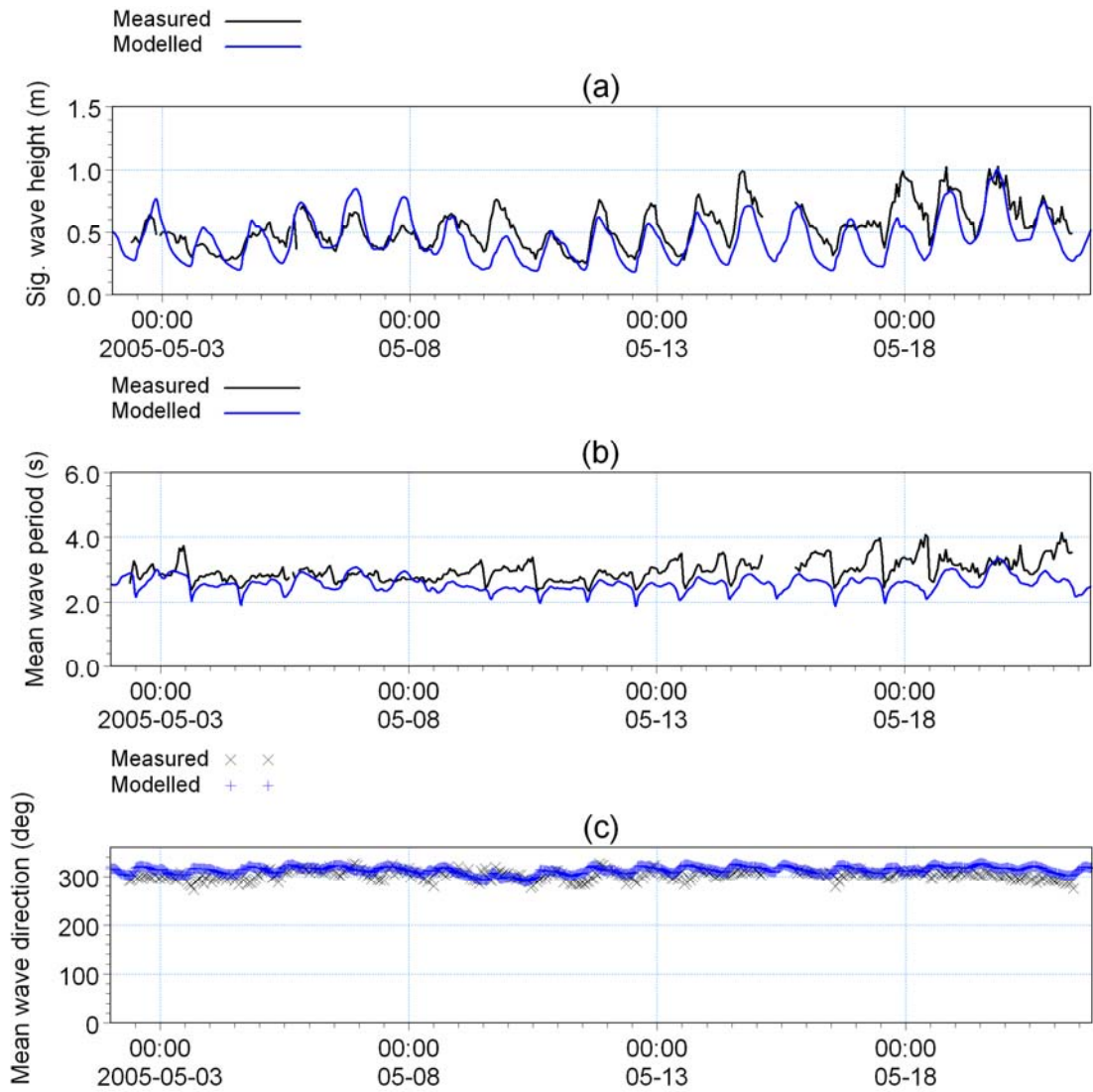


Figure 3-15. Comparison between measured and modelled wind sea parameters at B2: (a) significant wave height, (b) mean wave period and (c) mean wave direction.

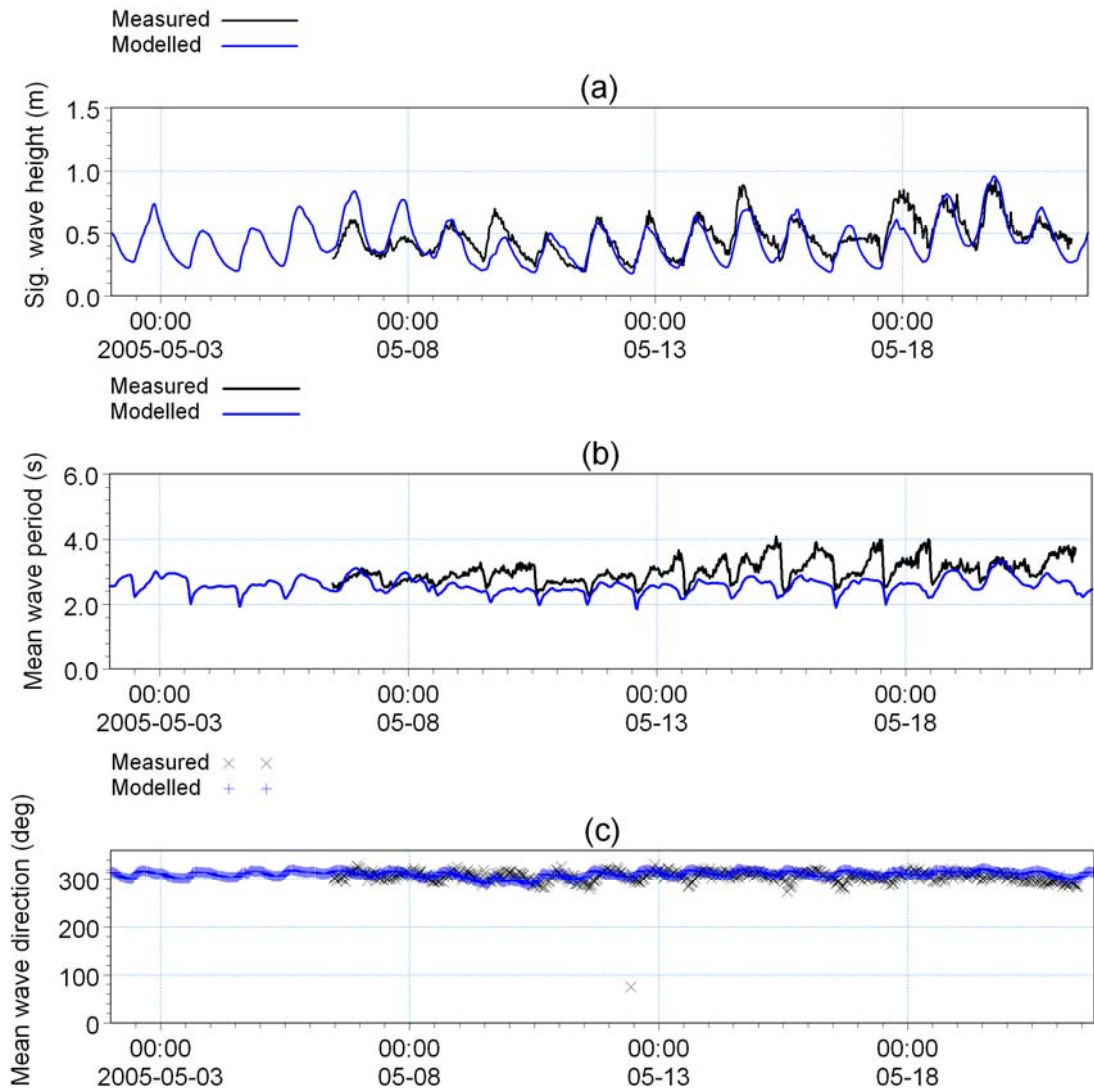


Figure 3-16. Comparison between measured and modelled wind sea parameters at B3: (a) significant wave height, (b) mean wave period and (c) mean wave direction.

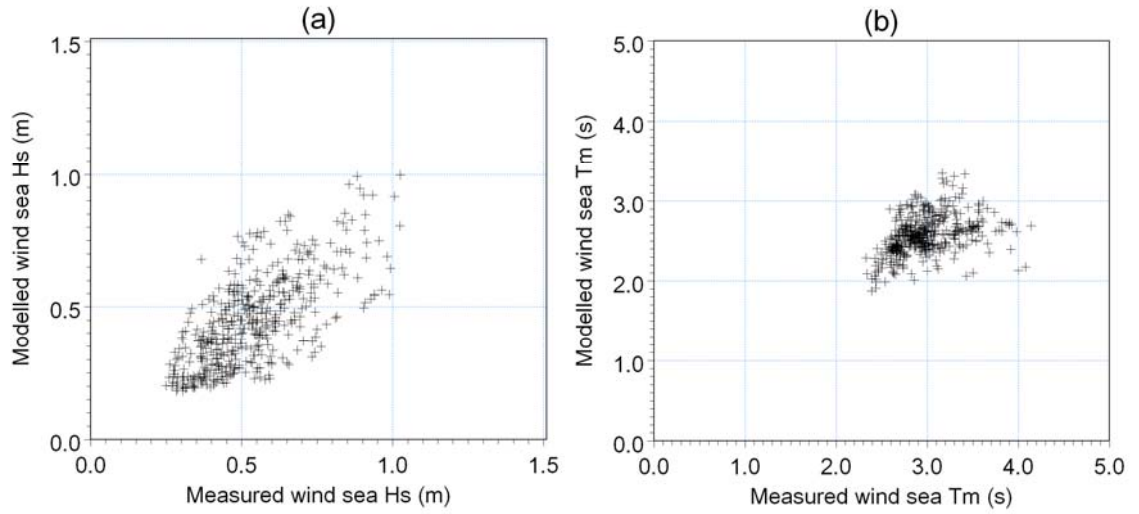


Figure 3-17. Scatter between measured and modelled (a) wind sea H_s and (b) wind sea T_m at B2.

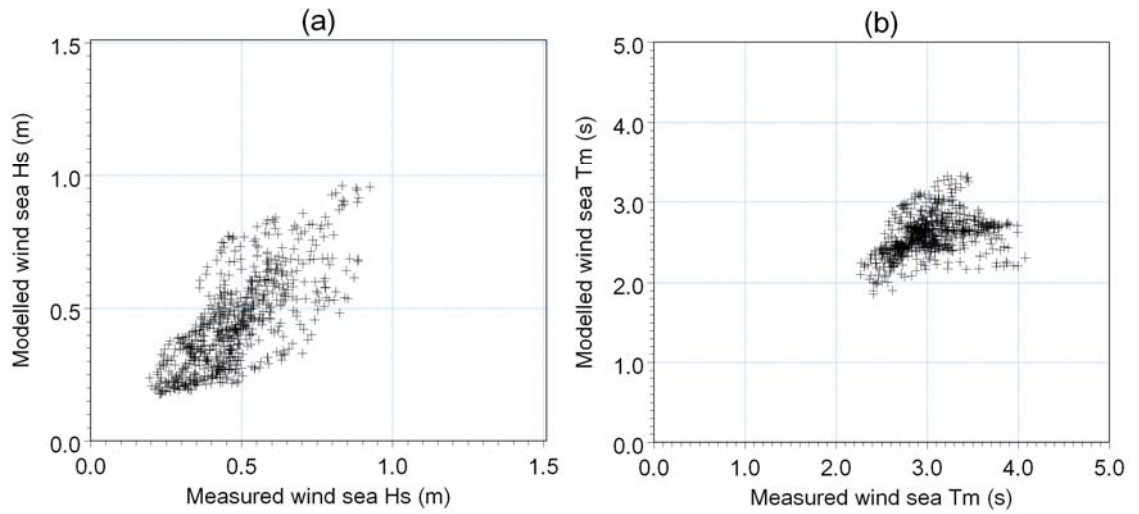


Figure 3-18. Scatter between measured and modelled (a) wind sea H_s and (b) wind sea T_m at B3.